

# Control of Vehicle Active Front Steering Based on Active Disturbance Rejection Feedback Controller

Sang Nan (桑楠)<sup>1,2\*</sup>, Wei Minxiang (魏民祥)<sup>1</sup>, Bai Yu (白玉)<sup>2</sup>

1. College of Energy and Power Engineering, Nanjing University of Aeronautics and Astronautics, Nanjing 210016, P. R. China;

2. College of Mechanical and Electrical Engineering, Changzhou Institute of Technology, Changzhou 213002, P. R. China

(Received 21 November 2014; revised 26 January 2015; accepted 28 February 2015)

**Abstract:** A control method of active front steering (AFS) based on active disturbance rejection technique was proposed for solving the model nonlinearity and parameter decoupling control in the traditional control methods. The AFS controller consists of the proportional and derivative (PD) feed-forward controller and the active disturbance rejection feedback controller. To improve the steering response characteristics of a vehicle, a PD controller is designed to realize variable steering gear ratio, and to enhance the safety of vehicle when steering. An active disturbance rejection controller (ADRC) is designed to follow the expected yaw rate of the vehicle. According to the input and output of system, extended state observer (ESO) of ADRC can dynamically estimate internal and external disturbance of the system, thus easily realizing the model nonlinear and parameter decoupling control. The AFS controller is simulated and validated in Matlab and CarSim. The simulating results of double lane change (DLC) test and pylon course slalom (PCS) test show that the ADRC can well control the vehicle model to complete the road simulation test of DLC and PCS with small path tracking error. The simulating results of angle step test of steering wheel show that the vehicle under the control of ADRC demonstrates good lateral response characteristic. The controller regulates a wide range of parameters. The model has less precision requirements with good robustness.

**Key words:** active disturbance rejection technique; active steering; variable ratio; extended state observer

**CLC number:** U461.4

**Document code:** A

**Article ID:** 1005-1120(2015)04-0461-08

## Nomenclature

|  |   |
|--|---|
| $m/\text{kg}$                          | Mass of vehicle                                 |
| $I_z/(\text{kg} \cdot \text{m}^2)$     | Moment of inertia about $Z$ -axis               |
| $k_1/(\text{N} \cdot \text{rad}^{-1})$ | Front axle cornering stiffness                  |
| $k_2/(\text{N} \cdot \text{rad}^{-1})$ | Rear axle cornering stiffness                   |
| $l_f/\text{m}$                         | Distance between CG and front axle              |
| $l_r/\text{m}$                         | Distance between CG and rear axle               |
| $\delta_{\text{sw}}/\text{rad}$        | Steering wheel angle                            |
| $\delta_{\text{FF}}/\text{rad}$        | Steering wheel angle of feed-forward            |
| $\delta_{\text{FB}}/\text{rad}$        | Steering wheel angle of feedback                |
| $\delta_p/\text{rad}$                  | Out angle of planetary gear trains              |
| $\theta_{\text{ac}}/\text{rad}$        | Angle of active front steering motor (actuator) |
| $\theta_p/\text{rad}$                  | Angle of 6-gear                                 |
| $\delta_f/\text{rad}$                  | Steer angle of front wheels                     |

|   |  |
|---|--|
| $n_i$                                     | Teeth of $i$ -gear                       |
| $\psi/(\text{rad} \cdot \text{s}^{-1})$   | Yaw rate                                 |
| $\psi_d/(\text{rad} \cdot \text{s}^{-1})$ | Yaw rate of reference model              |
| $\beta/\text{rad}$                        | Sideslip angle of vehicle centre of mass |
| $\beta_d/\text{rad}$                      | Sideslip angle of reference model        |
| $G$                                       | Mechanical steering gear ratio           |
| $u_x/(\text{m} \cdot \text{s}^{-1})$      | Longitudinal velocity                    |
| $g/(\text{m} \cdot \text{s}^{-2})$        | Acceleration due to gravity              |

## 0 Introduction

The traditional steering system completes the steering through the intervention of the driver. Therefore, it has the disadvantages of slow response speed, the incapability of correcting the driver's wrong operations, the helplessness in satisfying small gear ratio requirements at low speed

\* **Corresponding author:** Sang Nan, Associate Professor, E-mail: sangn@czu.cn.

**How to cite this article:** Sang Nan, Wei Minxiang, Bai Yu. Control of vehicle active front steering based on active disturbance rejection feedback controller[J]. Trans. Nanjing U. Aero. Astro., 2015,32(4):461-468.

<http://dx.doi.org/10.16356/j.1005-1120.2015.04.461>

and large gear ratio requirements at high speed, namely the so-called light and flexible contradiction. Owing to the small variation of gear ratio of traditional steering system, the steering characteristics of vehicle have nonlinear relations with vehicle speed. Therefore, the driver needs to constantly revise the vehicle direction to adapt to the steering characteristics of the vehicle so as to control the vehicle along the driver's desired track, which increases the driving burden and decreases the operability of the vehicle. Hydraulic power steering (HPS) or electric power steering (EPS) can change the transfer characteristics of steering force, but cannot change those of steering angle. Therefore, the problem that the vehicle steering characteristics change with the vehicle speed still exists. Active steering system was developed on the basis of power steering system, which includes active front steering (AFS), 4 wheels steering (4WS) and steering by wire (SBW), etc. A variable gear ratio (normalized steering gear ratio) can be realized by controlling the input of the active steering motor to get better steering performance, thus improving the handling and stability of vehicle and enhancing driving safety<sup>[1,2]</sup>.

The light and flexible contradiction can be solved by variable ratio of active steering. Based on the state of the vehicle, an additional angle is applied to the front wheels for changing the lateral force to ensure that the lateral dynamics meet the requirements. According to yaw rate and sideslip angle, the feed-forward controller implements abasic variable ratio rule based on vehicle speed, and the feedback controller adjusts wheel angle<sup>[3]</sup>. Steer gain (yaw rate gain or lateral acceleration gain) is invariable with velocity<sup>[4,5]</sup>; The variable ratio rule is amended based on invariable steer gain, and it is controlled by speed<sup>[6]</sup>. In fact, nonlinear characteristics of the tire, the vertical load and the suspension compliance will influence the actual angle of front wheels and change the relation between gear ratio and speed, so as to affect the vehicle steering characteristics. In this paper, basic variable gear ratio is realized by using proportional and derivative (PD) feed-forward

control, and the desired yaw rate is followed by using the active disturbance rejection control<sup>[7]</sup>. Known to the steering input and the output of vehicle (e. g. , steering angle, yaw rate, lateral acceleration, speed), active disturbance rejection controller (ADRC) can dynamically track targets. In order to verify the effectiveness of the proposed control methods, the drivers' commands are given by a single-point preview driver model and the driver-vehicle-road closed-loop control model is established in Matlab software. The CarSim vehicle model is controlled by this driver model to complete the road simulating test of high-speed double lane change (DLC) and pylon course slalom (PCS).

## 1 Variable Ratio Steering System Configuration and Model

### 1.1 Variable ratio steering system configuration

After adding the planetary gear mechanism in HPS or EPS, the variability of steering gear ratio was implemented by superposition of the movement of steering wheel and active front steering motor. Such system<sup>[8]</sup> was first applied in the BMW 5 series. The configuration of the variable ratio steering system is shown in Fig. 1.

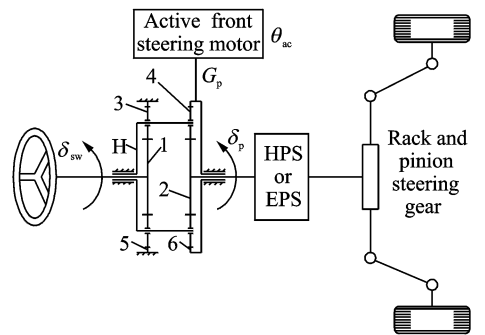


Fig. 1 Variable ratio steering system configuration

As shown in Fig. 1, while the steering system is working, the rotating direction of  $\delta_p$  and  $\delta_{sw}$  are the same, where  $G_p$  is the reduction ratio of motor and part 6,  $G_p = \theta_{ac}/\theta_p$ . Compound gear train has double row planetary gear train, including sun gears (part 1, 2, 5, 6), planet gears (part 3, 4) and planet carrier (part H), among which 5-sun gear is fixed. 1-3-H-5 is an elementa-

ry epicyclical gear train, 2-4-H-6 is a differential gear train, the system degree of freedom (DOF) is 2, and the output  $\delta_p$  is determined by  $\delta_{sw}$  and  $\theta_p$ . The relation among  $\delta_p$ ,  $\delta_{sw}$  and  $\theta_p$  satisfies

$$n_1 \delta_{sw} = n_1 \delta_p + n_5 \theta_p \quad (1)$$

From Eq. (1),  $\delta_p$  can be expressed as

$$\delta_p = \delta_{sw} - \theta_p \cdot n_5/n_1 \quad (2)$$

In this system, the mechanical steering gear ratio  $G$  was set to 17. The front wheel angle  $\delta_f$  equals to  $\delta_p/G$  and  $\alpha$  equals to  $n_5/n_1$ , then the vehicle steering gear ratio is defined as

$$i = \delta_{sw}/\delta_f = G \cdot \delta_{sw}/(\delta_{sw} - \alpha\theta_p) \quad (3)$$

When  $\theta_p = 0$ , then  $\delta_p = \delta_{sw}$ , the steering gear ratio  $i$  is constant. Active steering system becomes a constant ratio steering system. When  $\theta_p \neq 0$ ,  $i$  is determined by the values of  $\theta_p/\delta_{sw}$  as expressed in Eq. (3). Using the steering system as Fig. 1, steering variable gear ratio can be realized by controlling the input  $\theta_p$  or the actual control input  $\theta_{ac}$ .

Variable gear ratio can be realized by the active front steering shown in Fig. 1, and its control algorithm is shown in Fig. 2. According to the driver's input and vehicle speed, feed-forward controller calculates feed-forward steering wheel angle  $\delta_{FF}$ . According to  $\psi_d$ ,  $\beta_d$ ,  $\psi$  and  $\beta$ , feedback controller calculates feedback steering wheel angle  $\delta_{FB}$ . Feed-forward control algorithm is actually a proportional & derivative (PD) algorithm, and feedback control algorithm is an active disturbance rejection algorithm. In addition, one of the effects of the active steering control is that the response characteristic of the vehicle is changeable. This function is realized by feed-forward controller of the steering control, and the detailed algorithm will be described in Section 1.2. Another effect of the active steering control is that the vehicle response is less than the safety threshold. This function is realized by the feedback controller of the steering control, and the detailed algorithm will be described in Section 2.4.

## 1.2 Basic variable gear ratio control

The active front steering control system is designed to realize the functions mentioned above. The steering angle of the front wheel is deter-

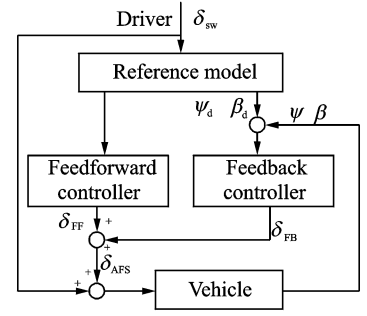


Fig. 2 Vehicle active steering control algorithm

mined by the driver and the actuator (motor). This angle can be controlled optionally by actively controlling the operating angle of the actuator. That is why the system is called the active front steering (AFS).

The relation among the front wheel angle, the actuator operating angle and the steering wheel angle is shown as follows<sup>[3]</sup>

$$\delta_f = (\delta_{sw} + \delta_{FF})/G \quad (4)$$

$\delta_{FF}$  is calculated as follows

$$\delta_{FF} = k_v \delta_{sw} + k_s \dot{\delta}_{sw} \quad (5)$$

where  $k_v$  is the proportional gain, and  $k_s$  the derivative gain.  $k_v$  and  $k_s$  are related to the speed of vehicle. Substituting  $\delta_{FF}$  of Eq. (5) into Eq. (4), its Laplace transform can be obtained.

$$\frac{\delta_{sw}}{\delta_f}(s) = \frac{G}{1 + k_v + k_s \cdot s} \quad (6)$$

where  $s$  is the Laplace operator. By setting up the relationships of  $k_v$  and  $k_s$  with the speed to realize the rules of basic variable gear ratio, the vehicle response characteristics can be actively controlled. In reference to BMW and Refs. [3, 9] about the range of the steering variable ratio and the relation between the variable ratio and the speed of vehicle, the kinematical function of the steering ratio is designed in this paper, as shown in Fig. 3.

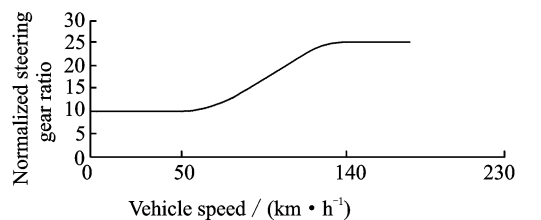


Fig. 3 Steering variable ratio rule

In active front steering as shown in Fig. 1, using control methods above, actual input of me-

chanical steering gear is  $\delta_p = \delta_{sw} + \delta_{FF} + \delta_{FB}$ . Compared with Eq. (2), the value of  $\theta_p$  can be determined, which equals to  $-(\delta_{FF} + \delta_{FB})n_1/n_5$ . Then, the expected variable gear ratio and steering characteristic can be realized by controlling the angle of active steering motor.  $\theta_{ac}$  can be expressed as

$$\theta_{ac} = -(\delta_{FF} + \delta_{FB})G_p n_1/n_5 \quad (7)$$

## 2 Driver-Vehicle-Road Closed-Loop Model

### 2.1 Driver model

Driver, vehicle and road are various aspects in the manipulation of vehicle. During driving, the driver has to constantly modify the vehicle direction according to the vehicle state and road conditions. The three aspects constitute a driver-vehicle-road closed-loop system. The "preview optimal curvature model"<sup>[10-12]</sup> proposed by Guo determines steering wheel angle based on single preview hypothesis and optimal curvature control. This model can simultaneously take the dynamic response characteristics of the vehicle and hysteresis of driver's response into account. It is called the single point preview driver model<sup>[10]</sup>, as shown in Fig. 4.

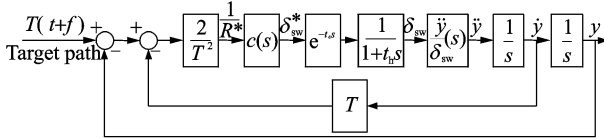


Fig. 4 Single point preview driver model

In Fig. 4,  $T$  is the preview time,  $c(s) = c_0(1 + T_c s)$ ,  $c_0 = u_x^2/G_{ay}$ , and  $G_{ay}$  is the steady-state gain of lateral acceleration. For a skilled driver,  $T$  can be set to 0.8 s,  $T_c$  0.406 8 s,  $t_d$  0.3 s, and  $t_h$  0.1s<sup>[9-11]</sup>. In actual application of the proposed model, the lateral speed and lateral displacement are given by the actual vehicle or the simulation model of the vehicle. In this paper, the drivers' input of the simulating vehicle is given by the single-point preview driver model.

### 2.2 Linear 2-DOF vehicle model

The 2-DOF linear vehicle model is commonly used in the study of steering movement (Fig. 5). The dynamic equation is described as<sup>[13]</sup>

$$\begin{cases} \dot{\psi} = \frac{l_f^2 k_1 + l_r^2 k_2}{I_z u_x} \psi + \frac{l_f k_1 - l_r k_2}{I_z} \beta - \frac{l_f k_1}{I_z} \delta_f \\ \dot{\beta} = \left( \frac{l_f k_1 - l_r k_2}{m u_x^2} - 1 \right) \psi + \frac{k_1 + k_2}{m u_x} \beta - \frac{k_1}{m u_x} \delta_f \end{cases} \quad (8)$$

Substituting  $\delta_f = (\delta_{sw} + \delta_{FF} + \delta_{FB})/G$  into Eq. (8), the following equations can be derived.

$$\dot{\psi} = f_{11}(\psi, \beta) + f_{12}(\delta_{sw}, \delta_{FF}) + b_1 \delta_{FB} \quad (9a)$$

$$\dot{\beta} = f_{21}(\psi, \beta) + f_{22}(\delta_{sw}, \delta_{FF}) + b_2 \delta_{FB} \quad (9b)$$

where  $f_{11}(\psi, \beta) = \frac{l_f^2 k_1 + l_r^2 k_2}{I_z u_x} \psi + \frac{l_f k_1 - l_r k_2}{I_z} \beta$

$$f_{21}(\psi, \beta) = \left( \frac{l_f k_1 - l_r k_2}{m u_x^2} - 1 \right) \psi + \frac{k_1 + k_2}{m u_x} \beta$$

$$f_{12}(\delta_{sw}, \delta_{FF}) = -\frac{l_f k_1}{G I_z} (\delta_{sw} + \delta_{FF})$$

$$f_{22}(\delta_{sw}, \delta_{FF}) = -\frac{k_1}{G m} (\delta_{sw} + \delta_{FF})$$

$$b_1 = -\frac{l_f k_1}{I_z G}, \quad b_2 = -\frac{k_1}{m G}$$

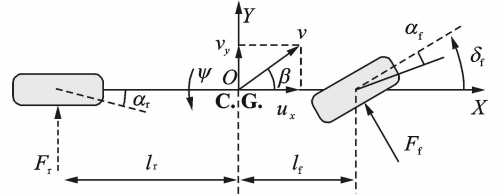


Fig. 5 2-DOF vehicle model

### 2.3 Reference model

The expected yaw rate  $\psi_d$  is determined by the desired linear 2-DOF model. Considering the road adhesion conditions of vehicle driving, the expected yaw rate response  $\psi_d$  on steering wheel under the angle input is expressed as

$$\psi_d = \frac{u_x/L}{(1 + K u_x^2)G} \delta_{sw} \quad |\psi_d| \leq \mu g/u_x \quad (10)$$

where  $K$  is the understeering coefficient of vehicle and  $\mu$  the adhesion coefficient of road.

### 2.4 Active disturbances rejection feedback controller

In this section, the design of ADRC<sup>[7]</sup> will be discussed in detail. ADRC is the feedback controller, and active angle  $\delta_{FB}$  operated by target yaw rate follow-up control. The actual vehicle model is much more complicated than the linear 2-DOF vehicle model with a lot of nonlinear problems. Obviously, compared with the actual vehicle mod-

el, the linear model of 2-DOF is over-simplified. Therefore, the proposed model contains a lot of unmodeled dynamics and its accuracy is poor. Control method depended on the precision of model is bad at the result control. The nonlinear coupling problem related to 2-DOF model requires a large amount of calculations to be decoupled. ADRC can adopt nonlinear feedback to implement dynamic compensation only based on the input and output of the system. Therefore, the first advantage of the ADRC model is that the control system can be treated by using a unified way, no matter the system is linear or nonlinear, certain or uncertain. The second advantage of the model is that in the rejection of disturbance, a specific and observable model for external disturbance is not necessary. Other advantages include: (1) The control algorithm does not need to identify the control object. (2) The control algorithm has good portability. (3) For the coupled problem of dynamic equation, only the static coupling need to be considered instead of the dynamic coupling.

Let  $\dot{x}_1 = xv_2 = \psi$ . Eq. (9a) can be expressed in the following two order system.

$$\begin{cases} \dot{x}_1 = x_2 \\ \dot{x}_2 = f_{11}(\psi, \beta) + f_{12}(\delta_{sw}, \delta_{FF}) + b_1 \delta_{FB} \\ y^* = x_1 \end{cases} \quad (11)$$

In Eq. (5),  $\hat{\delta}_{sw}$  can be obtained from  $\delta_{sw}$  by a differential process, which can be obtained from  $\delta_{sw}$  by a differential process. The method for obtaining  $\hat{\delta}_{sw}$  is

$$\begin{cases} fh = \text{Fhan}(v_1 - \delta_{sw}, v_2, r, h) \\ \dot{v}_1 = v_2, \quad \dot{v}_2 = fh \end{cases} \quad (12)$$

where the function  $\text{Fhan}(\cdot)$  is described by Eq. (2.4.6) in Ref. [7]. For the system described using Eq. (12), if  $|\dot{v}_1| \leq r$ , the parameter  $v_1$  can quickly track  $\delta_{sw}$ . Obviously, if  $v_1 \rightarrow \delta_{sw}$ , then  $v_2 \rightarrow \dot{\delta}_{sw}$ . Therefore, the system that Eq. (12) described is called the nonlinear tracking differentiator.

Similarly, the differential process mentioned above is adopted in the desired reference  $\psi_d$ , expressed in Eq. (13). This is called the transition process in ADRC technique. The first function is to increase the adjustable range of parameters;

the second function is to provide error signal for ADRC.

$$\begin{cases} fh = \text{Fhan}(v_1^* - \psi_d, v_2^*, r, h) \\ \dot{v}_1^* = v_2^*, \quad \dot{v}_2^* = fh \end{cases} \quad (13)$$

In Eq. (9a),  $f_{11}(\psi, \beta)$  is the sum of disturbance, which includes unmodeled error, parameter error and internal-external disturbance. Extended state observer (ESO) listed in Eq. (14) estimates the system states and the sum of disturbance.

$$\begin{cases} e = z_1 - y^* \\ fe = \text{Fal}(e, 0.5, \Delta) \\ fe_1 = \text{Fal}(e, 0.25, \Delta) \\ \dot{z}_1 = z_2 - \beta_{01}e \\ \dot{z}_2 = f_{12}(\delta_{sw}, \delta_{FF}) + z_3 - \beta_{02}fe + b_1 \delta_{FB} \\ \dot{z}_3 = -\beta_{03}fe_1 \end{cases} \quad (14)$$

where  $z_1$ ,  $z_2$ , and  $z_3$  estimate states  $x_1$ ,  $x_2$ , and  $x_3$ , respectively and  $x_3$  equals to  $f_{11}(\psi, \beta)$ . In Eq. (14), function  $\text{Fal}(\cdot)$  is expressed as

$$\text{Fal}(e, \xi, \Delta) = \begin{cases} |e|^\xi \text{sign}(e) & |e| > \Delta \\ e\Delta^{\xi-1} & |e| \leq \Delta \end{cases} \quad (15)$$

where  $\xi$  and  $\Delta$  are the positive numbers, and  $\text{sign}(\cdot)$  is the signum function.

The state errors of system  $e_1$  and  $e_2$  are defined as  $v_1 \cdot (-z_1)$  and  $v_2 \cdot (-z_2)$ , respectively, and they are used in the design of ADRC. In this paper, the feedback control law of error  $u_0$  is expressed as

$$\begin{aligned} u_0 &= \beta_1 \text{Fal}(e_1, \xi_1, \Delta) + \beta_2 \text{Fal}(e_2, \xi_2, \Delta) \\ 0 &< \xi_1 < 1 < \xi_2 \end{aligned} \quad (16)$$

In the ADRC algorithm,  $\delta_{FB}$  is dynamically calculated by ESO using  $u_0$  and  $z_3$ , expressed in Eq. (17).

$$\delta_{FB} = (u_0 - z_3 - f_{12}(\delta_{sw}, \delta_{FF})) / b_1 \quad (17)$$

where  $f_{12}$  is a known disturbance. Substituting  $\delta_{FB}$  of Eq. (17) into Eq. (14), the two-order ESO can be expressed as

$$\begin{cases} \dot{z}_1 = z_2 - \beta_{01}e \\ \dot{z}_2 = u_0 - \beta_{02}fe \end{cases} \quad (18)$$

Eq. (18) shows that ESO becomes a pure integrator tandem observer.  $\delta_{sw}$  is given by the driver model.  $\psi_d$  is obtained by the reference model and ESO is designed based on the linear 2-DOF model. Thanks to the fact that the nonlinear characteristics of model treated as disturbances are all included in  $f_{11}$ , ESO can guarantee enough preci-

sion.

So far, the ADRC and the PD controller have been discussed in this section and Section 1.2, respectively. According to the above discussion, the control model of AFS is shown in Fig. 6. Here, the ADRC controller is illustrated inside the dashed box in Fig. 6.

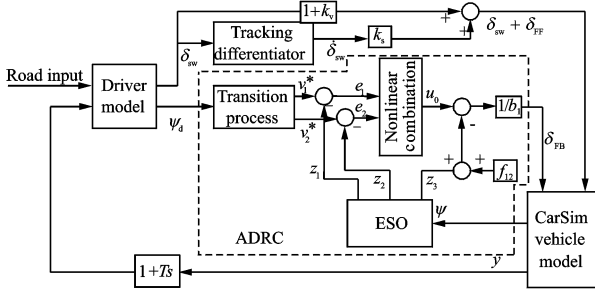


Fig. 6 Control model of active front steering

It can be seen from Eq. (8) that yaw rate  $\dot{\psi}$  and sideslip angle  $\beta$  are coupled. Using the ADRC controller, as long as  $y^*$  is measurable,  $f_{11}(\psi, \beta)$  can be estimated by  $z_3$  and the decoupling control of  $\psi$  and  $\beta$  is realized by ADRC without complex decoupling of matrix computation. Therefore, the algorithm of ADRC can ensure good real-time performance.

### 3 Simulation Analysis

In order to validate control effects of steering variable gear ratio and tracking performance of path of the proposed ADRC, a driver-vehicle-road closed-loop control model is established in Matlab/Simulink, which controls vehicle model of CarSim software (CS B-CLASS) to complete the tests of DLC and PCS. These two tests were carried out at speeds of 100 km/h and 120 km/h, respectively. The test path and placing of cones are adaptively set in accordance with the standard test<sup>[13,14]</sup> and the changes of speed (Technical Report of State Key Laboratory of Automobile Dynamic Simulation, Jilin University). Placing of cones for marking the pylon course slalom track is shown in Fig. 7, and that for marking the double lane-change track is shown in Fig. 8.

In Figs. 7,8, the center line of the trajectory surrounded by cones is a broken one, which is im-

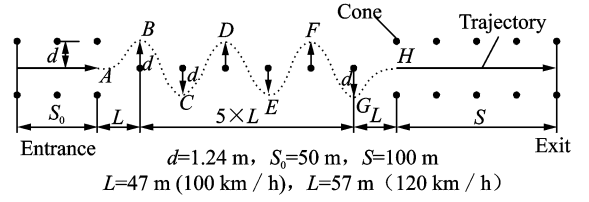


Fig. 7 Placing of cones for marking pylon course slalom track

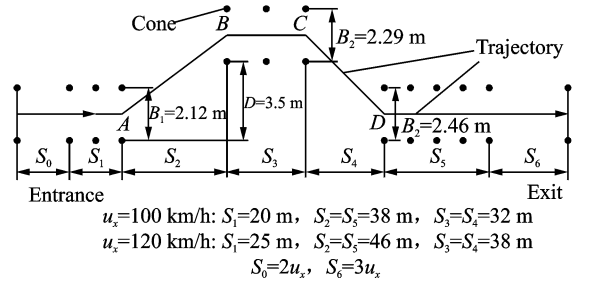


Fig. 8 Placing of cones for marking double lane-change track

possible for the vehicle to follow such a trajectory. Therefore, the non-smooth trajectory must be preview correction<sup>[11]</sup> in the simulation tests. The lines AB and GH in PCS test and the lines AB and CD in DLC test are replaced by cubic spline curves that satisfy the boundary conditions (The whole curve is smooth and continuous). The line B-G targeted trajectory in PCS test is a cosine curve, with the amplitude of  $d$ , as shown in Fig. 7. The parameters of simulation vehicle are listed in Table 1.

Table 1 Basic parameters of the vehicle

| Parameter   | Value   |
|---|---------|
| Mass of vehicle $m/\text{kg}$   | 1 231   |
| Distance between CG and front axle $l_f/\text{m}$                     | 1.04    |
| Distance between CG and rear axle $l_r/\text{m}$                      | 1.56    |
| Front axle cornering stiffness $k_1/(\text{N} \cdot \text{rad}^{-1})$ | 112 690 |
| Rear axle cornering stiffness $k_2/(\text{N} \cdot \text{rad}^{-1})$  | 112 690 |
| Moment of inertia about Z-axis $I_z/(\text{kg} \cdot \text{m}^2)$     | 2 331   |

The steering system of the existing vehicle has a feature of understeering to some degree. The actual vehicle model with a significant non-linear characteristic is controlled by the steering wheel angle derived from the simple driver model, which can track the ideal path at the beginning of the test. However, a large error appears at the later stage of the test, which is illustrated in the

simulating results in Figs. 9,10. In the test, road adhesion coefficient is 0.85. Since the vehicle exists understeering, if a vehicle bears no AFS, it is necessary for the driver to turn larger steering wheel angle to complete the test, as shown in Fig. 11. In such a test, the driver needs to constantly amend the steering angle, thus increasing driving difficulty. The results in Figs. 9,10 indicate

that the vehicle with AFS can perform the high-speed DLC and PCS tests well, and the path tracking performance is significantly better than that with the fixed gear ratio system. Moreover, it is not necessary for the driver to change his driving habit. The active front steering system can automatically compensate understeering and correct oversteering. Therefore, the driving difficulty is reduced, the handling and stability of vehicle are enhanced, and the driving safety is greatly improved.

For checking the performance of the ADRC model, the test of angle step input of steering wheel was conducted. The test results are shown in Fig. 12, where the solid line is the yaw rate step response curve without AFS, and the dashed line the yaw rate step response curve with AFS. The results in Fig. 12 show that the overshoot and the response time of yaw rate of the vehicle with AFS are obviously smaller than that without AFS. Hence, the response performance of vehicle with AFS is improved, which also indicates that AFS can improve the handling and stability of vehicle.

It is interesting that the same control parameters of ADRC are used to implement the DLC test, the PCS test and the step response test. The controlling effects of all tests are satisfying, which indicates that the ADRC controller has good robustness.

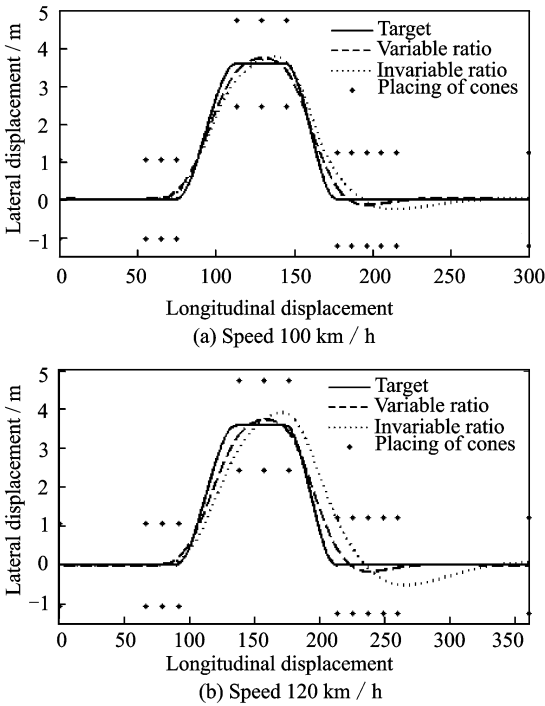


Fig. 9 High speed double lane change test

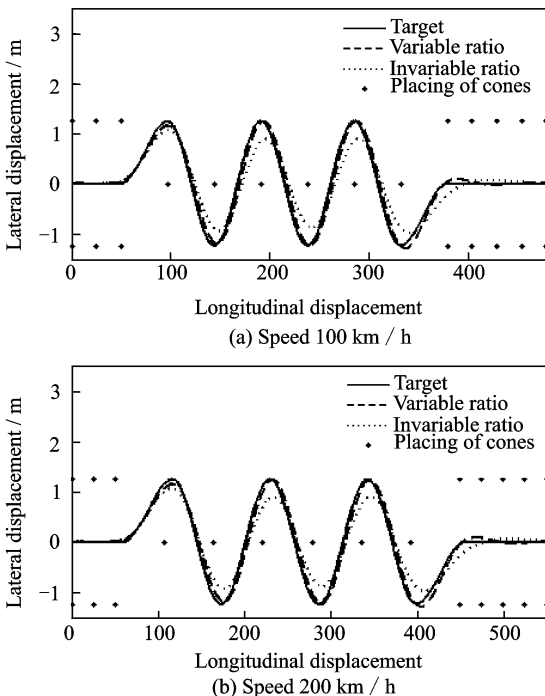


Fig. 10 High speed pylon course slalom test

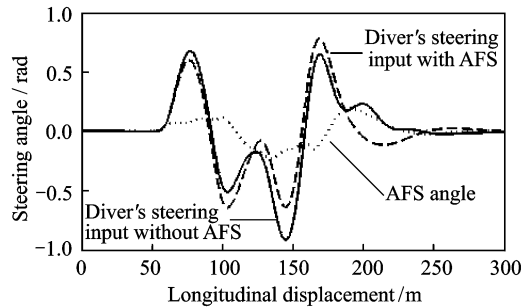


Fig. 11 Driver's input

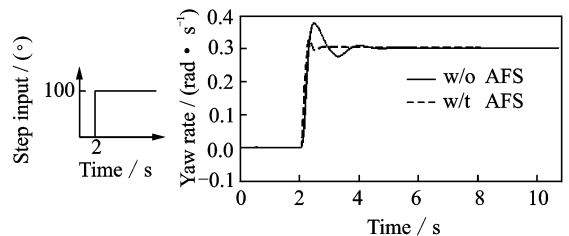


Fig. 12 Yaw rate step response

## 4 Conclusions

An AFS model of feed-forward control and feedback control is proposed. Feed-forward controller using the known PD algorithm has realized the changeable response characteristic of the vehicle. The feedback controller using active disturbance rejection technology has enhanced the controllability and stability of vehicle when steering. In the active disturbance rejection control, since the nonlinear characteristic of vehicle regarded as a disturbance can be estimated in real time and be dynamically compensated by ESO, the precise nonlinear dynamic equation is not necessary. The simulation results show that ADRC using 2-DOF model has good control effects. Here the nonlinear control problem and the decoupling problem of parameters are solved. Vehicle with AFS performs well in path tracking, characteristic of lateral response, and robustness.

Since the unmodeled dynamics, known or unknown disturbance and non-linear characteristic can be treated by using a unified way, the control method of ADRC is simple. Simultaneously, the design of ADRC controller does not need precise model and has no specific object, thus the controller has good the portability and adaptability.

The AFS without considering the influence of longitudinal force is investigated. In the ADRC controller designed for AFS the influence of longitudinal force, and the influences of suspension and other control system should be addressed in the further research, as well as the integrated control of AFS with other systems.

### Acknowledgement

This work was supported by the National Natural Science Foundation of China (No. 51205191).

### References:

- [1] Reinelt W, Klier W, Reimann G, et al. Active front steering (part 2): Safety and functionality[C]//SAE Technical Paper Series. USA: SAE Publication Group, Paper Number: 2004-01-1101.
- [2] Wang Chunyan, Zhao Wanzhong, et al. Parameter optimization of electric power steering integrated with active front steering function [J]. Transaction of Nanjing University of Aeronautics and Astronautics, 2012, 29(1): 96-102.
- [3] Kojo T, Suzumura M, Tsuchiya Y, et al. Development of active front steering control system[C]//SAE Technical Paper Series. USA: SAE Publication Group, Paper Number: 2005-01-0404.
- [4] Shang Gaogao, Hong Ze, Zhang hongdang, et al. Modeling of variable steering ratio with steady-state gain for active steering system [J]. Journal of Jiangsu University: Natural Science Edition, 2010, 31(3): 278-282. (in Chinese)
- [5] Liao Linqing, Wang Wei, Qu Xiang. Variable steer ratio of dynamic steering system based on yaw velocity gain[J]. Journal of Chongqing University of Technology: Natural Science Edition, 2011, 25(4): 1-5. (in Chinese)
- [6] Wei Jianwei, Wei Minxiang, Zhao Wanzhong. Control law of varied steering ratio based on driver-vehicle-road closed-loop system [J]. Journal of Jiangsu University: Natural Science Edition, 2011, 32(6): 652-657. (in Chinese)
- [7] Han Jingqing. Active disturbance rejection control technique the technique for estimating and compensating the uncertainties [M]. Beijing: National Defense Industry Press, 2008. (in Chinese)
- [8] Willy Klier, Wolfgang Reinelt. Active front steering (Part 1): Mathematical modeling and parameter estimation[C]//SAE Technical Paper Series. USA: SAE Publication Group, Paper Number: 2004-01-1102.
- [9] Jeonghoon Song. Design and evaluation of active front wheel steering system model and controller[C]//SAE Technical Paper Series. USA: SAE Publication Group, Paper Number: 2014-01-2000.
- [10] Guo K H. Drivers-vehiele closed-loop simulation of handling by "preselect optimal curvature method" [J]. Automotive Engineering, 1984, 3:1-16. (in Chinese)
- [11] Guo K H, Guan H. Modeling of driver / vehicle direction control system[J]. Vehicle System Dynamics, 1993, 22(3-4):141-184.
- [12] Guo K H. The principle of vehicle handling dynamics [M]. Nanjing: Science and Technology of Jiangsu Press, 2011. (in Chinese)
- [13] National Bureau of Technical Supervision. GB/T6323.1-94, Controllability and stability test procedure for automobiles Pylon course slalom test[S]. Beijing, 1994. (in Chinese)
- [14] International Standardization Organization. ISO/FDIS 3888-1, Passenger cars Test track for a severe lane change manoeuvre part 1: Double lane change[S]. Beijing, 1999.



